Transferred Nuclear Overhauser Effect Study of the C-Terminal Helix of Yeast Phosphoglycerate Kinase: NMR Solution Structure of the C-Terminal Bound Peptide

Marc Andrieux,[‡] Eric Leroy,[‡] Eric Guittet,*[,‡] Monica Ritco-Vonsovici,[§] Barbara Mouratou,[§] Philippe Minard,[§] Michel Desmadril,[§] and Jeannine M. Yon[§]

Laboratoire de RMN, Institut de Chimie des Substances Naturelles, Centre National de la Recherche Scientifique, 91190 F Gif sur Yvette, France, and Laboratoire d'Enzymologie Physicochimique et Moléculaire, Unité de Recherches du Centre National de la Recherche Scientifique, Université de Paris-Sud, 91405 F Orsay, France

Received August 3, 1994; Revised Manuscript Received November 7, 1994[⊗]

ABSTRACT: Two-dimensional ^{1}H nuclear magnetic resonance spectroscopy is used to determine the structure of the C-terminal complementary peptide (404−415) bound to a mutant phosphoglycerate kinase (1−403). Conformational changes in the peptide induced by the formation of the peptide−protein complex are followed by transferred nuclear Overhauser effect spectroscopy. Measurement of transferred NOEs and molecular modeling reveal an α-helix fold in the 405−409 region. This fold is in good agreement with the corresponding helix XIV of the crystallographic structure of wild-type PGK (Watson *et al.*, 1982). The role of the α-helix from the C-terminal peptide in the recovery of catalytic activity in the mutant PGK is discussed.

Many proteins have been found to fold with distinct structural regions called domains. Phosphoglycerate kinase (PGK)[1] is composed of two such globular domains, known as the N- and C-domains (Watson *et al.*, 1982). These two domains, of α/β structure, are linked together by an α-helical interdomain region composed of helices V, XIII, and XIV. Folding mechanisms of PGK have been widely studied and have pointed out the role of the interdomain helix XIV in the last phase of the folding process (Yon *et al.*, 1990; Ballery *et al.*, 1993).

In order to further investigate the role of this helix in the stability and folding of PGK, Minard and colleagues have produced and studied a mutant PGK obtained by removing the 12 last amino acids of the native protein. Complementation studies have shown that the C-terminal peptide induces a recovery of catalytic activity in the mutant PGK. On the basis of the dissociation constant value they determined (K_d = 80 μM), and assuming a k_{on} constant governed by a diffusional process, the k_{off} constant is estimated to be in the range 800−8000 s^{-1}. Such a value, in the fast exchange limit over the NMR time scale, led us to perform a TRNOESY study of the peptide in presence of yeast PGK Δ 404−415. TRNOESY is the extension of NOESY, which has been widely used to determine protein structures in solution (Wüthrich, 1986). At present, TRNOESY provides one of the best techniques for the determination of the structure of bound ligands in exchanging systems such as ligand−protein complexes (Campbell & Sykes, 1991a; Ni *et al.*, 1992; Lippens *et al.*, 1993). The intramolecular TRNOE allows the transfer of information concerning cross-relaxation between two nuclei in the bound ligand to the free ligand resonances via chemical exchange. In a rather coarse form, we can say that the free ligand "remembers" its bound conformation.

In order to understand the molecular basis of the biological measurements, we have determined the structure of the C-terminal peptide upon interaction with mutant PGK. By comparison with the crystallographic structure of native PGK, important features of the interaction are enlightened. The structural implications of the peptide−protein complex are inspected in terms of catalytic activity recovery.

MATERIALS AND METHODS

Peptide and Protein. HPLC-purified peptide (>95%) prepared by chemical synthesis was purchased from Neosystem (Strasbourg, France). Yeast PGK Δ 404−415 was prepared and purified according to Ritco-Vonsovici *et al.* (1995; see preceding paper). The purified protein was precipitated and stored in ammonium sulfate.

NMR Sample Preparation and Experiments. Yeast PGK Δ404−415 was dissolved in a 100 mM sodium acetate-d_3 (>99%, Aldrich Chimie, France) aqueous buffer, pH 6.4, and desalted on a Sephadex G25 column equilibrated with the same buffer. The concentration step of the protein was achieved using Amicon Centricon 30 microconcentrators. The protein concentration was measured by the UV absorbance at 278 nm using a molar extinction coefficient of 0.49 $(mg/mL)^{-1}$ cm^{-1}.

NMR experiments were performed on either a Bruker AM 400 or a Bruker AMX 600 spectrometer equipped for gradient spectroscopy with a sample consisting of 0.16 mM yeast PGK Δ 404−415, 2.85 mM peptide in 100 mM sodium acetate-d_3, and 95/5 H_2O/D_2O, pH 5.65, in a final volume of 0.55 mL. Assuming a dissociation constant of 80 × 10^{-6}

* To whom all correspondence should be addressed.
‡ Institut de Chimie des Substances Naturelles, CNRS.
§ Unité de Recherches du CNRS, Université de Paris-Sud.
⊗ Abstract published in *Advance ACS Abstracts,* December 15, 1994.
[1] Abbreviations: HPLC, high performance liquid chromatography; NMR, nuclear magnetic resonance; NOESY, nuclear Overhauser effect spectroscopy; PGK, phosphoglycerate kinase (EC 2.7.2.3); rmsd, root mean square deviation; ROESY, rotating Overhauser effect spectroscopy; TOCSY, total correlation spectroscopy; TRNOESY, transferred nuclear Overhauser effect spectroscopy; UV, ultraviolet.

0006-2960/95/0434-842$09.00/0

M (Ritco-Vonsovici *et al.*, accompanying paper), this leads to approximately 5% of the total peptide in the bound form. 2D NOESY (Ni, 1992; Ni *et al.*, 1992) and 2D ROESY (Griesinger & Ernst, 1987) spectra are recorded using a WATERGATE sequence (Piotto *et al.*, 1992; Sklenár *et al.*, 1993) for good water suppression. A spin-lock field of $\gamma B_1 = 9.49$ kHz was used in the ROESY experiments. Starting with the first t_1 point set at IN $- 4\tau_{90°}/\pi$, data sets of 511 by 2048 points were recorded with a sweep width of 6330 Hz, together with sine modulation and use of TPPI in both dimensions (Rance, 1989). The data were right-shifted by one point along the t_1 dimension, and the first missing FID was set to zero. One level of zero-filling and multiplication with shifted cosine or square cosine filters were applied in both dimensions prior to Fourier transformation. Base-line corrections were also applied using routines of the GIFA program (Delsuc, 1989; Rouh *et al.*, 1992). NOESY spectra were recorded with six different mixing times ranging from 50 to 240 ms. A Clean TOCSY spectrum (Griesinger *et al.*, 1988) with a 50 ms polarization transfer time was also recorded for spectral assignment. Spectra were recorded at 293 and 279 K on both spectrometers.

Derivation of Distance Constraints. Using the Felix program (Biosym Technologies, 1993), NOE distance constraints were derived from volume integration of a rectangular box defined around each peak on the 160 ms mixing time NOESY spectrum recorded at 279 K (Campbell & Sykes, 1991b). NOEs were sorted into three classes (strong, medium, weak) according to their relative intensities. Distance bounds for these classes were 2−2.6, 2.4−3.4, and 3.2−5 Å, respectively. Careful comparison of ROESY and NOESY spectra of the peptide in presence of protein was used in order to determine the contribution of the free peptide to the intensity of NOESY cross-peaks. When necessary, corrections for free ligand contribution were performed by increasing the initial upper distance bound to the upper bound value of the following intensity class.

Structure Determination. The full determination of the peptide structure consisted of a two stage protocol. First, NOE-derived distances, without lower distance bounds, were used as input for the DIANA program (Gunter *et al.*, 1991), using pseudo-atom corrections (Wüthrich, 1986). Structures having the best target function values were further minimized in a simulated annealing stage using the X-PLOR version 3.1 program (Brunger, 1992). This simulated annealing stage was a three step protocol (Bontems *et al.*, 1992) as follows: (i) The first step consisted of a 0.25 fs Verlet dynamic in a 0 K coupled bath followed by successive one step Powell minimizations with a stepwise decreasing harmonic potential applied on Cartesian coordinates; by the end of this level, the covalent geometry of the DIANA structures is regularized. (ii) The structures were then submitted to simulated annealing with 4 ps of soft thermalization to reach 1000 K followed by a 1 ps Verlet dynamic equilibration step. Then van der Waals radii were increased to their standard values in 10 steps of 2 ps each. A second 1 ps Verlet dynamic was applied in order to equilibrate the structures. Finally, the temperature was slowly decreased through 80 successive 0.5 ps Verlet dynamic stages. (iii) A final step was performed in order to lower the residual potential energy using a 0.25 ps Verlet dynamic in a 0 K coupled bath and with an explicit hydrogen bond energy term (Brunger, 1992), followed by a 5000 step Powell minimization. The experimental constraints were not included in stage i. Calculations were performed using the X-PLOR SUM option (Brunger, 1992) for the NOE potential. Slight corrections to upper NOE distance bounds were used: +0.8 Å for protons in isopropyl or aromatic groups, +0.3 Å for methyl groups.

Table 1: Proton Resonance Assignments of the Bound Peptide in Aqueous Solution at 279 K

	chemical shift[a] (ppm)			
residue	NH	αCH	βCH	others
E404		3.73	1.78	γCH_2 2.07
L405	8.72	4.34	1.30	γCH 1.42; δCH_3 0.65
P406		4.13	1.63, 2.02	γCH_2 1.75; δCH 3.39, 3.60
G407	8.35	3.69, 3.60		
V408	7.77	3.76	1.75	γCH_3 0.61
A409	8.25	3.98	1.01	
F410	8.06	4.27	2.78	δCH_2 6.95; ϵCH_2 7.07
L411	8.00	4.02	1.23	γCH 1.30; δCH_3 0.61, 0.54
S412	8.07	4.07	3.56	
E413	8.26	3.98	1.63	γCH_2 1.93, 2.00
K414	8.21	4.00	1.45	γCH_2 1.54; δCH_2 1.13
K415	7.98	3.88	1.41	γCH_2 1.53; δCH_3 1.11

[a] The chemical shift values are calibrated against the solvent proton resonance that was arbitrarily set to 4.80 ppm at 279 K.

RESULTS

NMR. (a) Preliminary Experiments. NOESY spectra (600 MHz) of the peptide alone displayed few weak positive cross-peaks at 279 K. Some sequential NOE peaks ($H\alpha_i$, NH_{i+1}) from residues Pro 3 to Glu 10 were present. Outside of the NH−Hα region, no interresidue correlations were observed. This small number of peaks can be explained either because the peptide adopts a loose and highly dynamic structure with no consistently short distances or by a molecular correlation time τ_c close to $1.11/\omega$ where the NOE is weak or null (ω = proton resonance frequency). In order to eliminate this second possibility, we performed control experiments at lower field and higher temperature values. When τ_c is lower than $1.11/\omega$, NOESY cross-peaks become negative with respect to diagonal peaks. However the same positive cross-peaks are observed on 400 MHz NOESY spectra at 293 K. These weak peaks correspond mainly to direct connectivity cross-peaks ($H\alpha_i$, NH_{i+1}), which are a common pattern of unstructured peptides in aqueous solution (Campbell & Sykes, 1991a) and are indicative of the absence of any secondary structure for the C-terminal peptide in the absence of PGK Δ404−415.

(b) Peptide Resonance Assignment. Sequential assignment of peptide resonances was carried out by combined use of NOESY and TOCSY spectra according to standard procedures (Wüthrich, 1986). This method relies on the observation of NOEs between the amide protons of one residue and the α protons, β protons, and amide protons of the preceding residue. Table 1 shows the ^1H chemical shifts for the resonances of the C-terminal peptide in presence of protein.

No change of the peptide resonances chemical shifts was observed upon binding to yeast PGK Δ404−415. This is due to the fact that the observed chemical shifts are dominated by the free ligand (Clore & Gronenborn, 1982; Campbell & Sykes, 1991a) which represents 95% of the total peptide concentration. In light of this bound/free ratio, only small changes of chemical shifts can appear since a 1 ppm modification in the bound peptide chemical shifts would lead to only a 0.05 ppm shift of the observed resonances. On

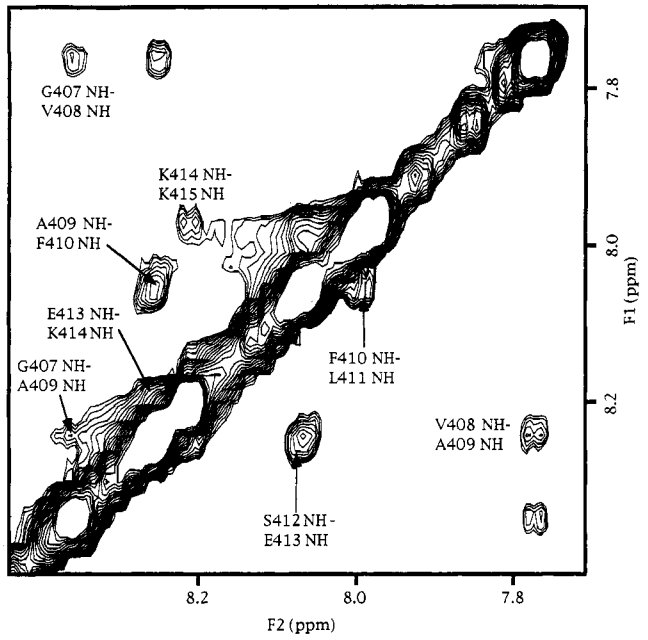

FIGURE 1: NH−NH region of the TRNOESY spectrum of the C-terminal peptide bound to yeast PGK Δ404−415. The spectrum was recorded with a mixing time of 200 ms at a temperature of 279 K.

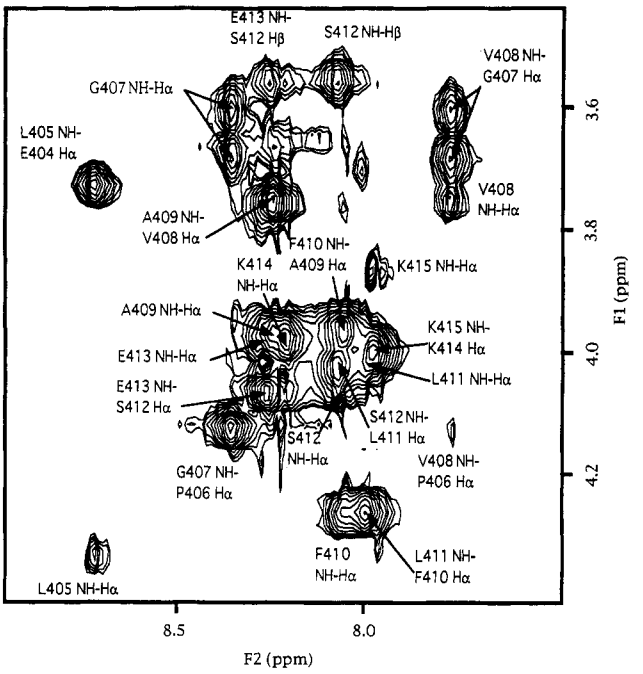

FIGURE 2: NH−Hα region of the TRNOESY spectrum of the C-terminal peptide bound to yeast PGK Δ404−415. The spectrum was obtained under the same experimental conditions as those in Figure 1. Unlabeled peaks arise from the protein.

the other hand, the line width is greatly influenced by the bound ligand. In the fast exchange limit, line broadening is expressed as follows (Campbell & Sykes, 1991a):

$$\frac{1}{T_2^{\text{obsd}}} = p\frac{1}{T_2^{\text{bound}}} + q\frac{1}{T_2^{\text{free}}}$$

where p and q are the relative proportions at each site ($p + q = 1$). T_2^{bound} is roughly proportional to the molecular weight of the ligand−protein complex. Therefore, $(1/T_2^{\text{bound}}) \gg (1/T_2^{\text{free}})$, and even with a low bound *versus* free ratio, line broadening could be observed. As expected, the peptide resonances undergo significant line broadening in presence of the protein.

The NOESY spectrum of the peptide displayed large modifications in the intensity and the number of peaks when the protein was added to the sample.

In the NH−NH correlation region, one can see the emergence of a new set of cross-peaks which sequentially connect the amide protons from residue 407 to residue 415 (see Figure 1). These peaks indicate spatial proximities of the amide protons, residues 407−410 being particulary intense. The emergence of these NH−NH cross-peaks is a fairly good indicator that a folding occurs under the bound state. One can also note the presence of a NH_i-NH_{i+2} correlation between residues Glu 407 and Ala 409. In the ROESY spectrum (data not shown), where the contribution of the free peptide is dominant, no NH−NH correlations can be distinguished above the noise. This confirms that the structural modifications affect the bound state only.

Figure 2 shows the NH−Hα region of the TRNOESY spectrum. The $H\alpha_i-NH_{i+1}$ correlations are visible, and one can also see the presence of a $H\alpha_i-NH_{i+2}$ peak between Pro 406 and Val 408.

Among the sequential restraints that define α-helical regions are those between sequential backbone NH residues and between backbone NH and Hβ protons of the preceding residue. Such strong $H\beta_i-NH_{i+1}$ cross-peaks are present from residues 406 to 409 (data not shown). Another helpful cross-peak in defining an α-helix is the medium-range restraint Pro406Hα−Ala409NH. From the set of correlations previously pointed out, it is clear that this segment displays a typical α-helix pattern on NOESY spectra.

Correlations between Leu405Hα and Pro406Hδδ′ reveal a Proline trans conformation (Wüthrich, 1986). From 411 to 415 residues, only sequential NOEs appear and are not indicative of a well-defined secondary structure.

In the TRNOE spectrum, we can see cross-peaks arising from the protein (unlabeled peaks in Figure 2). In a NOE spectrum of the PGK Δ404−415 (data not shown), it is possible to identify some of these sequential cross-peaks which arise from the N and C terminus of the protein. These NOEs are indicative of very mobile regions in the mutant PGK. However, no intermolecular NOE correlations between the peptide and these regions of the protein are found in the TRNOESY spectrum of the complex.

(c) Distance Determination. The interproton distances of the peptide in the bound state were derived from the pure phase absorption two-dimensional NOESY spectrum recorded with a mixing time of 160 ms. A set of 114 distance restraints was used for structure determination. They were sorted into three classes with appropriate corrections, as defined in Materials and Methods.

Structure Determination. A total of 1000 structures were generated using the DIANA program. The 20 best structures were selected according to their target function value and were refined using X-PLOR protocols, as described in Materials and Methods. At this point of the structure determination, it was possible to undertake stereospecific assignments in order to adjust the experimental set of constraints. This adjustment was carried out on the β and δ protons of proline 406 and the α protons of glycine 407. The two protons of each geminal pair had NOE cross-peaks

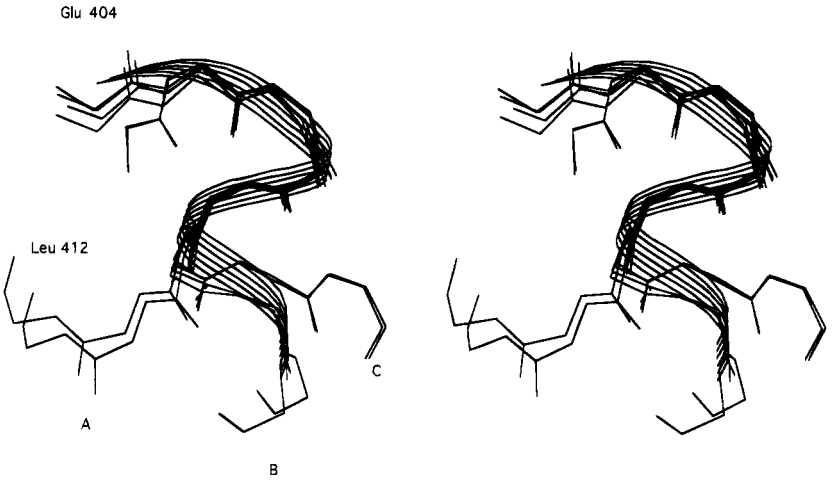

FIGURE 3: Stereo diagram of 6 final peptide structures. The backbone of peptides and a ribbon representation of the X-ray structure of PGK have been drawn for clarity. The superposition was carried out using the backbone atoms of the 405−409 region of the PGK. The displayed sequence of amino acids is from residue 404 to residue 412. Note the three possible orientations of the peptide tail labeled A, B, and C.

of different intensities to neighboring protons. Statistical examination of the best DIANA structures permitted the stereospecific assignment of each proton. It was also possible to confirm the presence of an α-helix within the 405−409 residues, as expected on NOESY spectra. Three new DIANA runs of 1000 structures each were carried out using this redefined set of upper bound restraints (i.e., including the new stereospecific restraints). Three sets of 20 structures were selected under a target function value criterion. These 60 selected structures were then submitted to two parallel runs of X-PLOR refinement. The differences between each run consisted in the presence (or absence) of nonexperimental dihedral restraints. In one run only the experimental constraints were used, and in the other run a set of φ angle restraints were added which restricted ($-80° \leq \varphi \leq -40°$) for four residues (Pro 406, Gly 407, Val 408, Ala 409). These φ angle values correspond to standard values from an α-helical conformation and were employed since NMR evidence and preliminary DIANA calculations had confirmed such a secondary structure. Both runs led to very similar results in term of structural conformations and energy values, except that the convergence of structures was better when the dihedral restraints were included in the refinement protocol. Thus, the results we present below relate to the structures refined with the dihedral angle constraints. Twenty-two structures among the 60 refined structures were selected according to their energy term values and their low number of distance restraints violation. None of these 22 structures exhibited distance violations greater than 0.25 Å, beyond the upper or lower bound limits. An average of only 3.6 ± 1.2 distance violations inferior to 0.25 Å were observed per structure (from the set of 114 distance restraints). As such, the structures presented a good agreement with the experimental constraints. They also were in good agreement with the ideal covalent geometry (results not shown). The 22 structures were clearly similar with averaged pairwise rmsd values of 2.8 ± 1.2 and 4.3 ± 1.3 Å for the backbone atoms and for all non-hydrogen atoms, respectively. In fact, these values give a poor idea of the convergence of the structures compared to the averaged pairwise rmsd values observed for the two regions of the peptide. For the 405−409 residues, the α-helix region, the averaged pairwise rmsd values were 0.44 ± 0.2 and 0.75 ± 0.3 Å for the backbone atoms and for all non-hydrogen atoms, respectively. Similarly, the 410−415 region was rather well-defined and presented averaged pairwise rmsd values of only 1.33 ± 0.4 and 3.53 ± 0.9 Å for the backbone atoms and for all non-hydrogen atoms, respectively. A lack of NOE restraints between the α-helix region and the 410−415 region explains the increase of the averaged pairwise rmsd values when considering the entire peptide.

Comparison with the X-ray Structure of the C-Terminal Peptide. To understand further the structural modification of the C-terminal peptide upon binding, it is worthwhile to compare our solution structures with the corresponding region in the X-ray structure of the wild-type yeast PGK.

In Figure 3 we show the superposition of 6 representative NMR-derived peptide structures on the 405−409 region of the crystallographic structure. One can see good agreement between NMR and X-ray structures in the α-helix region. The averaged rmsd values between the 22 selected structures and the X-ray structure are 0.58 ± 0.1 Å (backbone atoms) and 0.86 ± 0.1 Å (non-hydrogen atoms) for this region. Outside of the α-helix, the solution structures diverge from the crystallographic structure. The 410−415 region presents in solution three different orientations. Some structures are roughly oriented as the X-ray backbone (B), while others are left- (A) or right-oriented (C) as can be seen on Figure 3. These orientations represent three possible geometries for the C-terminal peptide tail. On the basis of NOESY spectra and molecular structure calculations, none of them can be excluded.

DISCUSSION AND CONCLUSION

NOESY spectra of the peptide/yeast PGK Δ404−415 complex display a huge increase in the number and intensities of peptide cross-peaks compared to the spectra of the peptide alone. Such an increase indicates a longer peptide correlation time which cannot be simply explained by an increase in viscosity of the solution due to the protein concentration (0.16 mM). This clearly implies the existence of peptide bound to the protein where dipolar relaxation phenomena are much more efficient due to their τ_c dependence. In this bound state, the peptide undergoes strong structural modifications in the 405−409 region. This region folds into an α-helix and presents good agreement with the X-ray structure of the helix XIV in the native PGK. We can conclude that upon

binding the peptide tends to recover a kind of "native" conformation. This structural analogy leads us to think that binding may occur at the native position of the helix XIV. This hypothesis is supported by biological considerations. Previous work (Ritco-Vonsovici *et al.*, preceding paper) has suggested great structural flexibility in PGK Δ404−415. This may be related to the flexibility observed in the isolated N- and C-domains from yeast PGK (Fairbrother *et al.*, 1989). Lack of contact between these two domains induces a destabilization of the overall protein structure. The interdomain region plays an important role in the the stability and the catalytic activity of the protein. Mas and Resplandor (1988) have emphazised the contribution of α-helices XIII and XIV to the stability of the "basic patch" region, i.e., His 62, His 167, His 170, Arg 21, Arg 38, Arg 65, and Arg 168, which forms part of the native PGK active site (Watson *et al.*, 1982; Walker *et al.*, 1989). In the absence of the stabilizing contribution of α-helix XIV, mutant PGK displays a very low activity level (0.1% of the native enzymatic activity). Upon binding at the native helix XIV position, the C-terminal peptide induces a kind of packing of the N-domain leading to a correct rearrangement of the active site. The 3-phosphoglycerate binding to PGK also requires interactions with the amino end of interdomain helix XIII. Among well-resolved resonances of yeast PGK Δ404−415, some of them arise from 398−403 residues and lead to NOE cross-peaks (NOESY spectrum of yeast PGK Δ404−415, data not shown). These peaks are indicative of a higher flexibility region with regard to the overall protein. The NOESY spectrum of this part of the protein displays sequential $H\alpha_i-NH_{i+1}$ cross-peaks and no NH−NH correlation. It is likely that helix XIII (393−401) is greatly destabilized and by this means alters the 3-phosphoglycerate binding site. Nevertheless, the catalytic activity of the peptide−protein complex represents a 40-fold increase in yeast PGK Δ404−415 enzymatic activity, demonstrating the crucial role of the C-terminal helix in the catalytic activity of yeast PGK (Ritco-Vonsovici *et al.*, preceding paper).

Superposition of the C-terminal peptide on helix XIV X-ray structure displays a good convergence on this section. However, in the crystallographic structure, Phe 410 belongs to this helix. On the NMR structure, no spectral evidence may lead us to the same conclusion. The set of peptide structures shows the possibility of three different orientations of the 411−415 region compared to the helix region (see Figure 3). Phe 410, which links these two regions, seems to act as a pivot for the three orientations mentioned above. Choosing one orientation of the aromatic ring would allow definition of one preferential orientation of the peptide tail. However, it is not possible to conclude from the NOE constraints only. One way to solve this problem is to carry out a structural refinement in the presence of protein. Molecular modeling of the C-terminal peptide in its binding site will allow us to better understand the structural constraints of the interaction. Such a work is in progress and will be reported later.

In conclusion, we have demonstrated on the basis of TRNOESY spectra that an interaction between the peptide and yeast PGK Δ404−415 occurs. Overall peptide correlations are indicative of a conformational change upon binding. This folding as an α-helix suggests strong homology with the corresponding region in the X-ray structure of the wild-type enzyme. The recovery of enzymatic activity demonstrates the key role of helix XIV in the activity of yeast PGK. This structural and biological information suggests to us that the peptide binding site is probably the native position of yeast PGK helix XIV. It should also be noted that some conformational changes must occur in yeast PGK Δ404−415 upon binding of the peptide in order to restore an active catalytic site. This underlines the fact that binding is a dynamic process with mutual changes in the structure of the two partners.

REFERENCES

Ballery, N., Desmadril, M., Minard, P., & Yon, J. M. (1993) *Biochemistry 32*, 708−714.

Bontems, F., Gilquin, B., Roumestand, C., Ménez, A., & Toma, F. (1992) *Biochemistry 31*, 7756−7764.

Brünger, A. T. (1992) *X-PLOR version 3.1*, Yale University Press, New Haven.

Campbell, A. P., & Sykes, B. D. (1991a) *J. Mol. Biol. 222*, 405−421.

Campbell, A. P., & Sykes, B. D. (1991b) *J. Magn. Reson. 93*, 77−92.

Clore, G. M., & Gronenborn, A. M. (1982) *J. Magn. Reson. 48*, 402−417.

Delsuc, M. A. (1989) in *Maximum Entropy and Bayesian Methods* (Skilling, J., Ed.) pp 285−290, Kluwer Academic, Dordrecht, The Netherlands.

Fairbrother, W. J., Minard, P., Hall, L., Betton, J. M., Missiakas, D., Yon, J. M., & Williams, R. J. P. (1989) *Protein Eng. 3*, 5−11.

Felix version 2.3 (1993) Biosym Technologies, San Diego.

Griesinger, C., & Ernst, R. R. (1987) *J. Magn. Reson. 75*, 261−271.

Griesinger, C., Otting, G., Wüthrich, K., & Ernst, R. R. (1988) *J. Am. Chem. Soc. 110*, 7870−7872.

Günter, P., Braun, W., & Wüthrich, K. (1991) *J. Mol. Biol. 217*, 517−530.

Lippens, G., Hallenga, K., Van Belle, D., Wodak, S. J., Nirmala, N. R., Hill, P., Russell, K. C., Smith, D. D., & Hruby, V. J. (1993) *Biochemistry 32*, 9423−9434.

Mas, M. T., & Resplandor, Z. E. (1988) *Proteins: Struct., Funct., Genet. 4*, 56−62.

Ni, F. (1992) *J. Magn. Reson. 100*, 391−400.

Ni, F., Ripoll, D. R., Martin, P. D., & Edwards, B. F. P. (1992) *Biochemistry 31*, 11551−11557.

Piotto, M., Saudek, V., & Sklenar, V. (1992) *J. Biomol. NMR 2*, 661−665.

Rance, M. (1989) *Bruker Users Meeting*, Billerica, MA.

Ritco-Vonsovici, M., Mouratou, B., Minard, P., Desmadril, M., Yon, J. M., Andrieux, M., Leroy, E., & Guittet, E. (1995) *Biochemistry 34*, 833−841.

Rouh, A., Delsuc, M. A., Bertrand, G., & Lallemand, J. Y. (1993) *J. Magn. Reson., Ser. A 102*, 357−359.

Sklenar, V., Piotto, M., Leppik, R., & Saudek, V. (1993) *J. Magn. Reson., Ser. A 102*, 241−245.

Walker, P. A., Littelchild, J. A., Hall, L & Watson, H. C. (1989) *Eur. J. Biochem. 183*, 49−55.

Watson, H. C., Walker, N. P. C., Shaw, P. J., Bryant, T. N., Wendell, P. J., Fothergill, L. A., Perkins, R. E., Conroy, S. C., Dobson, M. J., Tuite, M. F., Kingsman, A. J., & Kingsman, S. M. (1982) *EMBO J. 1*, 1635−1640.

Wüthrich, K. (1986) *NMR of Proteins and Nucleic Acids*, Wiley & Sons, New York.

Yon, J. M., Desmadril, M., Minard, P., Ballery, N., Missiakas, D., Gaillard-Miran, S., Perahia, D., & Mouawad, L. (1990) *Biochimie 72*, 417−429.

BI9417832